E-Companion

Title: Emergency Drone Deployment and Disposable Defibrillator Allocation: A Modular Capacitated Maximum Covering Location Model.

Authors: Run Zhang, Fangfang Wu, Xiandong Zhang, Bo Chen

EC.1 Tractable reformulation of the DRO model

Recall that the MC-MCLP-DR problem contains worst-case functions in both the objective and constraint. We replace the objective function with an auxiliary variable γ, so that the uncertainty objective is moved to constraints, and we reformulate the problem as

$$\text{MC-MCLP-}\gamma: \min_{(\boldsymbol{x},\boldsymbol{y},\boldsymbol{k})\in\mathcal{X},\gamma} \quad \gamma \tag{A.1a}$$

$$\text{s.t.} \quad \sup_{\mathbb{P}\in\mathcal{G}} \mathbb{E}_{\mathbb{P}} \sum_{i\in\mathcal{I}} \tilde{a}_i (1 - \sum_{j\in\mathcal{N}_i} x_{ij}) \leq \gamma \tag{A.1b}$$

$$\inf_{\mathbb{P}\in\mathcal{G}} \mathbb{P}\left[\max_{j\in\mathcal{J}} (\sum_{i\in\mathcal{M}_j} \tilde{a}_i x_{ij} - k_j)^+ < U\right] \geq R_0 \tag{A.1c}$$

Here, constraint (A.1b) is a semi-infinite qualifier that the constraint should hold for all probability, i.e.,

$$\sup_{\mathbb{P}\in\mathcal{G}} \mathbb{E}_{\mathbb{P}} \sum_{i\in\mathcal{I}} \tilde{a}_i (1 - \sum_{j\in\mathcal{N}_i} x_{ij}) \leq \gamma \Longleftrightarrow \mathbb{E}_{\mathbb{P}} \sum_{i\in\mathcal{I}} \tilde{a}_i (1 - \sum_{j\in\mathcal{N}_i} x_{ij}) \leq \gamma, \forall\, \mathbb{P}\in\mathcal{G}.$$

Therefore, MC-MCLP-γ is a semi-infinite program, which is known to not have a direct solution. We aim to reformulate this as an optimization problem that can be solved using an off-the-shelf solver. To this end, we use the dual method in Section EC.1.1 to solve the problem through dualization of the left-side worst-case functions in (A.1b) and (A.1c). Specifically, given allocation $\boldsymbol{x}$ of demand area and disposable AED capacity assignment $\boldsymbol{k}$, we transform each worst-case function to a regular robust optimization problem, and reformulate it as a linear programming problem as in Propositions EC.1 and EC.2. The supremum/infimum in the original MC-MCLP-γ problem can be replaced by an infimum/supremum, and the reformulated constraint should hold for at least one corresponding solution in the dual space. We incorporate the two propositions in the overall MC-MCLP-γ model, which becomes a nonlinear programming problem (containing a bilinear term) in Lemma EC.3. In Section EC.1.2, the nonlinear programming model is linearized as mixed integer linear programming (MILP) by the BigM method.

EC.1.1 Reformulation of the worst-case functions

There are two types of worst-case functions in the MC-MCLP-γ problem: the worst-case uncovering demand function and the worst-case probability constraint function. Recall that (A.2) is an objective function in MC-MCLP-DR. We use the concept of the objective function for context consistency as well as to more easily distinguish it with the probability constraint. The two types of functions are:

$$\sup_{\mathbb{P}\in\mathcal{G}} \mathbb{E}_{\mathbb{P}} \sum_{i\in\mathcal{I}} \tilde{a}_i(1-\sum_{j\in\mathcal{N}_i} x_{ij}) \tag{A.2}$$

$$\inf_{\mathbb{P}\in\mathcal{G}} \mathbb{P}\left[\max_{j\in\mathcal{J}}(\sum_{i\in\mathcal{M}_j} \tilde{a}_i x_{ij} - k_j) < U\right], \tag{A.3}$$

where the demand area allocation $\boldsymbol{x}$ and disposable AED capacity assignment $\boldsymbol{k}$ are given. Example 1 is used as the $g(\cdot)$ function in $\mathcal{G}$. We first develop an equivalent formulation of regular robust optimization for the worst-case objective function (A.2). Based on the formulation, disposable AED capacity assignment $\boldsymbol{k}$ is not related to worst-case objective function (A.2); hence only the demand area allocation $\boldsymbol{x}$ is needed. Lemma EC.1 presents the first-step formulation.

LEMMA EC.1. *Given demand assignment decision* $\boldsymbol{x}$*, the worst-case objective function* (A.2) *is equivalent to the optimal value of the following optimization problem:*

$$\min_{\boldsymbol{\alpha}\le\mathbf{0},\boldsymbol{\beta},\boldsymbol{\lambda}\ge\mathbf{0},\tau\in\mathbb{R}} \sum_{i\in\mathcal{I}} \left(\alpha_i\underline{\mu}_i + \beta_i\overline{\mu}_i\right) + \boldsymbol{\lambda}^\top\boldsymbol{\delta} + \tau \tag{A.4a}$$

$$\text{s.t.} \sum_{i\in\mathcal{I}} a_i\left(\alpha_i+\beta_i\right) + \boldsymbol{w}^\top\boldsymbol{\lambda} + \tau \ge \sum_{i\in\mathcal{I}} a_i(1-\sum_{j\in\mathcal{N}_i} x_{ij}), \forall\ (\boldsymbol{a},\boldsymbol{w})\in\mathcal{W} \tag{A.4b}$$

where $\boldsymbol{\alpha},\boldsymbol{\beta},\boldsymbol{\lambda},\tau$ *are auxiliary variables.*

Problem (A.4) is a semi-infinite-dimensional optimization problem because of the infinity realization of $(\boldsymbol{a},\boldsymbol{w})$ in set $\mathcal{W}$ create infinite constraints in (A.4), which cannot be solved directly. With the duality argument, this semi-infinite problem can be transformed to the linear programming problem (A.5), which is computationally tractable. Proposition EC.1 shows the transformation.

PROPOSITION EC.1. *Given decision* $\boldsymbol{x}$ *and Example 1 as a function* $g(\cdot)$*, the worst-case objective function* (A.2) *is equivalent to the following linear programming problem:*

$$\min \sum_{i\in\mathcal{I}} \left(\alpha_i\underline{\mu}_i + \beta_i\overline{\mu}_i\right) + \boldsymbol{\lambda}^\top\boldsymbol{\delta} + \tau \tag{A.5a}$$

$$\text{s.t.}\ -\tau \le \sum_{i\in\mathcal{I}} (c_i\underline{a}_i + e_i\overline{a}_i + f_i\mu_i^a - g_i\mu_i^a) \tag{A.5b}$$

$$c_i + e_i + f_i - g_i \le \alpha_i + \beta_i - (1-\sum_{j\in\mathcal{N}_i} x_{ij}), \forall\ i\in\mathcal{I} \tag{A.5c}$$

$$-f_i - g_i \le \lambda_i, \forall\ i\in\mathcal{I} \tag{A.5d}$$

$$\boldsymbol{\alpha}\le 0, \boldsymbol{\beta},\boldsymbol{\lambda}\ge\mathbf{0}, \tau\in\mathbb{R}; \quad \boldsymbol{c}\ge\boldsymbol{0}, \boldsymbol{e},\boldsymbol{f},\boldsymbol{g}\le\boldsymbol{0}, \tag{A.5e}$$

where $\boldsymbol{\alpha},\boldsymbol{\beta},\boldsymbol{\lambda},\tau,\boldsymbol{c},\boldsymbol{e},\boldsymbol{f},\boldsymbol{g}$ *are auxiliary variables.*

We next establish an equivalent formulation for the worst-case probability function (A.3). Similar to a technique in Wang et al. (2020), for each potential location $j\in\mathcal{J}$, we denote an intersection set,

$$\mathcal{A}_j(\boldsymbol{x},\boldsymbol{k}) = \left\{\boldsymbol{a}\in R^{|I|}\ \middle|\ \sum_{i\in\mathcal{M}_j} \tilde{a}_i x_{ij} - k_j < U\right\} \bigcap \left\{\boldsymbol{a}\in R^{|\mathcal{I}|}\ \mid\ 0 < U\ \right\}, \tag{A.6}$$

where the backup volume U satisfies $U > 0$. A complementary set of $\mathcal{A}_j(\boldsymbol{x}, \boldsymbol{k})$ is

$$\overline{\mathcal{A}}_j(\boldsymbol{x}, \boldsymbol{k}) = \left\{ \boldsymbol{a} \in R^{|I|} \;\middle|\; \sum_{i \in \mathcal{M}_j} \tilde{a}_i x_{ij} - k_j \geq U \right\}. \tag{A.7}$$

With the notation in (A.6), the worst-case probabilistic function (A.3) can be written in terms of the probability of its event $\inf_{\mathbb{P} \in \mathcal{G}} \mathbb{P}\Big[\cap_{j \in \mathcal{J}} (\tilde{\boldsymbol{a}}, \tilde{\boldsymbol{w}}) \in \mathcal{A}_j(\boldsymbol{x}, \boldsymbol{k}) \Big]$. We define the set of events $\mathcal{E} := \cap_{j \in \mathcal{J}} (\tilde{\boldsymbol{a}}, \tilde{\boldsymbol{w}}) \in \mathcal{A}_j(\boldsymbol{x}, \boldsymbol{k})$, and rewrite (A.3) as

$$\inf_{\mathbb{P} \in \mathcal{G}} \mathbb{P}\Big[\mathcal{E}\Big] = \inf_{\mathbb{P} \in \mathcal{G}} (1 - \mathbb{P}\Big[\overline{\mathcal{E}}\Big]) = 1 - \sup_{\mathbb{P} \in \mathcal{G}} \mathbb{P}\Big[\overline{\mathcal{E}}\Big]. \tag{A.8}$$

The first equality holds from the probability definition. The second keeps the optimal value and distribution solution unchanged. The complementary event $\overline{\mathcal{E}}$ can be explicitly written in terms of De Morgan's laws as

$$\overline{\mathcal{E}} = \overline{\cap_{j \in \mathcal{J}} \{(\tilde{\boldsymbol{a}}, \tilde{\boldsymbol{w}}) \in \mathcal{A}_j(\boldsymbol{x}, \boldsymbol{k})\}} = \cup_{j \in \mathcal{J}} \{(\tilde{\boldsymbol{a}}, \tilde{\boldsymbol{w}}) \in \overline{\mathcal{A}}_j(\boldsymbol{x}, \boldsymbol{k})\}. \tag{A.9}$$

Then we incorporate (A.9) in (A.8) to obtain two equivalent expressions of probability function (A.3):

$$\text{(A.3)} = \inf_{\mathbb{P} \in \mathcal{G}} \mathbb{P}\Big[\cap_{j \in \mathcal{J}} \{(\tilde{\boldsymbol{a}}, \tilde{\boldsymbol{w}}) \in \mathcal{A}_j(\boldsymbol{x}, \boldsymbol{k})\} \Big] = 1 - \sup_{\mathbb{P} \in \mathcal{G}} \mathbb{P}\Big[\cup_{j \in \mathcal{J}} \{(\tilde{\boldsymbol{a}}, \tilde{\boldsymbol{w}}) \in \overline{\mathcal{A}}_j(\boldsymbol{x}, \boldsymbol{k})\} \Big]. \tag{A.10}$$

Using the last equivalent expression in (A.10), we reformulate the probability function (A.3) as a semi-infinite optimization problem in Lemma EC.2, and reformulate this as a linear programming in Proposition EC.2.

LEMMA EC.2. *Given defibrillation demand area assignment decision $\boldsymbol{x}$ and disposable AED capacity allocation $\boldsymbol{k}$, the worst-case probability function* (A.3) *is equivalent to the optimal value of the following optimization problem:*

$$\max_{\boldsymbol{\alpha}' \leq \boldsymbol{0}, \boldsymbol{\beta}', \boldsymbol{\lambda}' \geq \boldsymbol{0}, \tau' \in \mathbb{R}} \; 1 - \sum_{i \in \mathcal{I}} \left(\alpha_i' \underline{\mu}_i + \beta_i' \overline{\mu}_i \right) - \boldsymbol{\lambda}'^\top \boldsymbol{\delta} - \tau' \tag{A.11a}$$

$$\text{s.t.} \sum_{i \in \mathcal{I}} a_i (\alpha_i' + \beta_i') + \boldsymbol{w}^\top \boldsymbol{\lambda}' + \tau' \geq 1, \; \forall \; (\boldsymbol{a}, \boldsymbol{w}) \in \mathcal{W} \cap \overline{\mathcal{A}}_j(\boldsymbol{x}, \boldsymbol{k}), \forall \; j \in \mathcal{J} \tag{A.11b}$$

$$\sum_{i \in \mathcal{I}} a_i (\alpha_i' + \beta_i') + \boldsymbol{w}^\top \boldsymbol{\lambda}' + \tau' \geq 0, \; \forall \; (\boldsymbol{a}, \boldsymbol{w}) \in \mathcal{W} \tag{A.11c}$$

where $\boldsymbol{\alpha}', \boldsymbol{\beta}', \boldsymbol{\lambda}', \tau'$ are auxiliary variables.

The derived optimization problem (A.11) is still semi-infinite-dimensional, and hence is not directly solvable. By a duality argument, we linearize it as (A.12).

PROPOSITION EC.2. *Given demand allocation $\boldsymbol{x}$, capacity assignment decisions $\boldsymbol{k}$, and function $g(\cdot)$ as in Example 1, the value of the worst-case probability function* (A.3) *is equivalent to a linear programming problem:*

$$\max \; 1 - \sum_{i \in \mathcal{I}} \left(\alpha_i' \underline{\mu}_i + \beta_i' \overline{\mu}_i \right) - \boldsymbol{\lambda}'^\top \boldsymbol{\delta} - \tau' \tag{A.12a}$$

$$\text{s.t. } 1-\tau' \leq h^j(U+k_j)+\sum\nolimits_{i\in\mathcal{I}}(\underline{a}_i l_i^j+\overline{a}_i m_i^j+\mu_i^a n_i^j-\mu_i^a o_i^j), \forall\ j\in\mathcal{J} \tag{A.12b}$$

$$x_{ij}h^j+l_i^j+m_i^j+n_i^j-o_i^j \leq (\alpha_i'+\beta_i'), \forall\ j\in\mathcal{J}, i\in\mathcal{M}_j \tag{A.12c}$$

$$l_i^j+m_i^j+n_i^j-o_i^j \leq (\alpha_i'+\beta_i'), \forall\ j\in\mathcal{J}, i\in\mathcal{I}/\mathcal{M}_j \tag{A.12d}$$

$$-n_i^j-o_i^j \leq \lambda_i', \forall\ j\in\mathcal{J}, i\in\mathcal{I} \tag{A.12e}$$

$$-\tau' \leq \sum\nolimits_{i\in\mathcal{I}}(\underline{a}_i r_i+\overline{a}_i s_i+\mu_i^a t_i-\mu_i^a\zeta_i) \tag{A.12f}$$

$$r_i+s_i+t_i-\zeta_i \leq (\alpha_i'+\beta_i'), \forall\ i\in\mathcal{I} \tag{A.12g}$$

$$-t_i-\zeta_i \leq \lambda_i', \forall\ i\in\mathcal{I} \tag{A.12h}$$

$$\boldsymbol{\alpha}' \leq \mathbf{0}, \boldsymbol{\beta}', \boldsymbol{\lambda}' \geq \mathbf{0}, \tau'\in\mathbb{R} \tag{A.12i}$$

$$\boldsymbol{r}\geq \mathbf{0}, \boldsymbol{s}\leq\mathbf{0}, \boldsymbol{t}\leq\mathbf{0}, \boldsymbol{\zeta}\leq\mathbf{0};\quad \boldsymbol{h}\geq\mathbf{0}, \boldsymbol{l}\geq\mathbf{0}, \boldsymbol{m}\leq\mathbf{0}, \boldsymbol{n}\leq\mathbf{0}, \boldsymbol{o}\leq\mathbf{0} \tag{A.12j}$$

where $\boldsymbol{h}, \boldsymbol{l}, \boldsymbol{m}, \boldsymbol{n}, \boldsymbol{o}, \boldsymbol{\alpha}', \boldsymbol{\beta}', \boldsymbol{\lambda}', \tau', \boldsymbol{r}, \boldsymbol{s}, \boldsymbol{t}, \boldsymbol{\zeta}$ *are auxiliary variables.*

In the overall MC-MCLP-γ problem, the uncertainty is incorporated in constraints (A.1b) and (A.1c), and it involves two worst-case functions, (A.2) and (A.3). In Propositions EC.1 and EC.2, we obtain the equivalent optimization problems (A.5) and (A.12) for (A.2) and (A.3), respectively. Here, the two constraints hold for at least one corresponding solution in the feasible space of (A.5) and (A.12). Thus, the linear optimization problem (A.5) and (A.12) can be directly incorporated in MC-MCLP-γ. Hence we have Lemma EC.3, which is an equivalent nonlinear programming for MC-MCLP-γ (and MC-MCLP-DR).

LEMMA EC.3. *Given* $g(\cdot)$ *function as in Example 1, the* MC-MCLP-DR *problem is equivalent to a mixed integer bilinear programming problem:*

$$\text{MC-MCLP-MIBP: } \min\ \gamma$$

$$\text{s.t. } \sum\nolimits_{i\in\mathcal{I}}\left(\alpha_i\underline{\mu}_i+\beta_i\overline{\mu}_i\right)+\boldsymbol{\lambda}^\top\boldsymbol{\delta}+\tau\leq\gamma \tag{A.13a}$$

$$1-\sum\nolimits_{i\in\mathcal{I}}\left(\alpha_i'\underline{\mu}_i+\beta_i'\overline{\mu}_i\right)-\boldsymbol{\lambda}'^\top\boldsymbol{\delta}-\tau'\geq R_0 \tag{A.13b}$$

$$1-\tau' \leq h^j(U+k_j)+\sum\nolimits_{i\in\mathcal{I}}(\underline{a}_i l_i^j+\overline{a}_i m_i^j+\mu_i^a n_i^j+\mu_i^a o_i^j), \forall\ j\in\mathcal{J}$$

$$h^j x_{ij}+l_i^j+m_i^j+n_i^j-o_i^j \leq (\alpha_i'+\beta_i'), \forall\ j\in\mathcal{J}, i\in\mathcal{M}_j$$

$$\text{(A.5b)}-\text{(A.5e)}, \text{(A.12d)}-\text{(A.12j)};\quad (\boldsymbol{x},\boldsymbol{y},\boldsymbol{k})\in\mathcal{X}, \gamma\in\mathbb{R},$$

where $\gamma, \boldsymbol{\alpha}, \boldsymbol{\beta}, \boldsymbol{\lambda}, \tau, \boldsymbol{c}, \boldsymbol{e}, \boldsymbol{f}, \boldsymbol{g}, \boldsymbol{h}, \boldsymbol{l}, \boldsymbol{m}, \boldsymbol{n}, \boldsymbol{o}, \boldsymbol{\alpha}', \boldsymbol{\beta}', \boldsymbol{\lambda}', \tau', \boldsymbol{r}, \boldsymbol{s}, \boldsymbol{t}, \boldsymbol{\zeta}$ *are auxiliary variables.*

Note that (A.12) is a linear programming problem given $\boldsymbol{x}$ and $\boldsymbol{k}$ in Proposition EC.2. However, as demand assignment $\boldsymbol{x}$ and capacity assignment $\boldsymbol{k}$ are decision variables in the MC-MCLP-MIBP problem, there exist non-convex bilinear terms such as $h_j x_{ij}$ and $h_j k_j$, making it difficult to find a global optimal solution, We mitigate this with a BigM method.

EC.1.2 Linearization on bilinear terms and an MILP

We linearize the nonlinear term by a combination of integer branching and the classical BigM method. Recall that the MIBP problem contains separate bilinear terms of variables $\boldsymbol{x}$ and $\boldsymbol{k}$, and that $\boldsymbol{k}$ is a vector of integer variables and cannot directly be used with a BigM method. Hence we branch the integer variable based on a set of new binary variables, where special order set branching is often used (Yang et al. 2021). We use a type 1 Special Ordered Set (Special ordered sets were introduced for modeling nonconvex problems. A type 1 special ordered set asks that at most one element from an ordered set can have a nonzero value.) to replace the integers $k_j, \forall\ j \in \mathcal{J}$, as binary variables. The product of a binary and continuous variable can be linearized using the BigM method. For each location j, we assume there exits a maximal disposable AED capacity assignment k_j^U and minimal disposable AED assignment k_j^L of location capacity; then the assignment of capacity value satisfies $k_j \in \{0, k_j^L, k_j^L+1, ...k_j^U\}$. Hence the capacity allocation $\boldsymbol{k}$ can be linearized as

$$k_j = \sum\nolimits_{t=k_j^L}^{k_j^U} t z_t^j + 0 z_0^j \ \text{ s.t. } \sum\nolimits_{t=k_j^L}^{k_j^U} z_t^j + z_0^j = 1,\ \forall\ j \in \mathcal{J},$$

where the z_t^j are new binary decision variables that represent capacity volume acquires t. Moreover, z_0^j satisfies $z_0^j + y_j = 1$ by definition. Thus, we equivalently linearize the expression of the bilinear terms $h^j(U + k_j), \forall\ j \in \mathcal{J}$:

$$\begin{aligned} h^j(U+k_j) &= h^j(U + \sum\nolimits_{t=k_j^L}^{k_j^U} t z_t^j) \\ & s.t.\ \ \sum\nolimits_{t=k_j^L}^{k_j^U} t z_t^j = k_j, \forall\ j \in \mathcal{J} \text{ and } \sum\nolimits_{t=k_j^L}^{k_j^U} z_t^j = y_j, \forall\ j \in \mathcal{J}, \end{aligned} \tag{A.14}$$

where the bilinear terms contain binary variables $\boldsymbol{z}$ and continuous variables $\boldsymbol{h}$. To use the BigM method, we first note the dual variables $h^j, \forall\ j \in \mathcal{J}$ are bounded. Then we introduce new auxiliary variables $\kappa_t^{1j}, \kappa_{ij}^2 \geq 0$ to replace the bilinear terms $h^j z_t^j$ and $x_{ij} h^j$ through a sufficiently large constant M (an upper bound value of variable h^j) and linearized formulations. The linearized constraints for all $\mathcal{J}$ are:

$$\begin{aligned} &\kappa_t^{1j} \leq M z_t^j, \forall\ t \in \{0, k_j^L, ..., k_j^U\}, j \in \mathcal{J} && \kappa_{ij}^2 \leq M x_{ij}, \forall\ i \in \mathcal{M}_j, j \in \mathcal{J} \\ &\kappa_t^{1j} \leq h^j, \forall\ t \in \{0, k_j^L, ...,, k_j^U\}, j \in \mathcal{J} && \kappa_{ij}^2 \leq h^j, \forall\ i \in \mathcal{M}_j, j \in \mathcal{J} \\ &\kappa_t^{1j} \geq h^j - M(1 - z_t^j), \forall\ t \in \{0, k_j^L, ..., k_j^U\}, j \in \mathcal{J} && \kappa_{ij}^2 \geq h^j - M(1 - x_{ij}), \forall\ i \in \mathcal{M}_j, j \in \mathcal{J}, \end{aligned} \tag{A.15}$$

where the nonlinear term is overcome, and a formulation of MILP is derived for the distributionally robust capacitated covering location problem (MC-MCLP-DR).

LEMMA EC.4. *Given Example 1 as a function $g(\cdot)$, MC-MCLP-DR is equivalent to the following mixed integer linear programming problem:*

$$\text{MC-MCLP-MILP:} \min\ \gamma \tag{A.16a}$$

$$\text{s.t. (A.13a)} - \text{(A.13b)}$$

$$1 - \tau' \leq Uh^j + \sum\nolimits_{t=k_j^L}^{k_j^U} t\kappa_t^{1j}$$
$$+ \sum\nolimits_{i\in\mathcal{I}} (\underline{a}_i l_i^j + \overline{a}_i m_i^j + \mu_i^a n_i^j + \mu_i^a o_i^j), \forall\ j \in \mathcal{J} \quad \text{(A.16b)}$$
$$\kappa_{ij}^2 + l_i^j + m_i^j + n_i^j - o_i^j \leq (\alpha_i' + \beta_i'), \forall\ j \in \mathcal{J}, i \in \mathcal{M}_j \quad \text{(A.16c)}$$
$$\text{(A.5b)} - \text{(A.5e)}, \text{(A.12d)} - \text{(A.12j)}, \text{(A.14)}, \text{(A.15)}, \quad (\boldsymbol{x}, \boldsymbol{y}, \boldsymbol{k}) \in \mathcal{X}, \quad \text{(A.16d)}$$

where $\gamma, \boldsymbol{\alpha}, \boldsymbol{\beta}, \boldsymbol{\lambda}, \tau, \boldsymbol{c}, \boldsymbol{e}, \boldsymbol{f}, \boldsymbol{g}, \boldsymbol{h}, \boldsymbol{l}, \boldsymbol{m}, \boldsymbol{n}, \boldsymbol{o}, \boldsymbol{\alpha}', \boldsymbol{\beta}', \boldsymbol{\lambda}', \tau', \boldsymbol{r}, \boldsymbol{s}, \boldsymbol{t}, \boldsymbol{z}$ *are auxiliary variables.*

EC.2 Methods for accelerating computation

We present three types of methods to improve the solvability of the MC-MCLP-MILP formulation. We derive valid lower and upper bound inequalities, present two families of symmetry-breaking constraints, and determine lower bounds of BigM.

EC.2.1 Valid inequalities

We derive lower and upper bounds for auxiliary variables using the structure of the proposed model. These are used when we reformulate the worst-case objective and constraint function. The solution of $\boldsymbol{\alpha}', \boldsymbol{\beta}', \boldsymbol{\lambda}', \tau'$ must satisfy

$$\tau' \geq -\sum_{i\in\mathcal{I}} \mu_i^a (\alpha_i' + \beta_i'), \qquad -\sum_{i\in\mathcal{I}} \left(\frac{\mu_i^a}{\overline{\mu}_i - \mu_i^a}\right) \leq \tau' \leq 1 + \sum_{i\in\mathcal{I}} \left(\frac{\underline{\mu}_i}{\mu_i^a - \underline{\mu}_i}\right),$$
$$0 \leq \alpha_i' \left(\underline{\mu}_i - \mu_i^a\right) \leq 1 \Longrightarrow \frac{-1}{\mu_i^a - \underline{\mu}_i} \leq \alpha_i' \leq 0, \qquad 0 \leq \lambda'_i \delta_i \leq 1 \Longrightarrow 0 \leq \lambda'_i \leq \frac{1}{\delta_i},$$
$$0 \leq \beta_i' (\overline{\mu}_i - \mu_i^a) \leq 1 \Longrightarrow 0 \leq \beta_i' \leq \frac{1}{\overline{\mu}_i - \mu_i^a}.$$

EC.2.2 Symmetry breaking

We derive two types of symmetry breaking constraints to reduce the feasible region of decision variables.

EC.2.2.1 Representation of integer variables

In Section EC.1.2, the integer variable was represented by the type 1 Special Order Set. Here, we describe the integer $k_j, \forall\ j \in \mathcal{J}$, using binary variables in a more direct manner. Symmetry breaking constraints are specifically designed for the problems under consideration (Shehadeh et al. 2019). To accelerate computing, we also use binary variables to incorporate the symmetry structure and break it.

As in the literature, for each location j, we assume both an upper and lower bound on the location disposable AED value assignment, and the assignment satisfies $k_j \in \{0, k_j^L, k_j^L + 1, \ldots, k_j^U\}$. Thus, the integer $\boldsymbol{k}$ can be described as $k_j = z_{k_j^L}^j k_j^L + \sum\nolimits_{t=k_j^L+1}^{k_j^U} z_t^j$ s.t. $z_{k_j^L}^j = y_j, \forall\ j \in \mathcal{J}$, where z_t^j is a new binary decision variable that defines capacity volume acquires one unit indexed in t. In this way, we linearize the expression of the bilinear terms $h^j(U+k_j), \forall\, j \in \mathcal{J}$, as $h^j(U+z^j_{k^L_j}k^L_j+\sum_{t=k^L_j+1}^{k^U_j} z^j_t), \forall\, j \in \mathcal{J}$, such that

$$k_j = z^j_{k^L_j}k^L_j + \sum_{t=k^L_j+1}^{k^U_j} z^j_t \ , \ z^j_{k^L_j} = y_j \text{ and } \sum_{t=k^L_j+1}^{k^U_j} z^j_t \le (k^U_j - k^L_j + 1)y_j, \ \forall\, j \in \mathcal{J}. \tag{A.18}$$

Different from the linearized bilinear term (A.14) in MC-MCLP-MILP, (A.18) enables interchanging of two homogeneous disposable AED with no difference in term value. This motivates us to introduce the symmetry-breaking constraints to reduce the solution space. In (A.18), the bilinear term contains $\boldsymbol{z}$. The dual variables $h^j, \forall\, j \in \mathcal{J}$, are bounded (see Section EC.1.2, and we know that the dual problem of the bilinear problem is bounded and has a nonempty interior, the proof of Proposition EC.2. We also introduce a sufficiently large constant M (the upper bound of variable h^j) and a linearized formulation by replacing $h^j z^j_t$ and $x_{ij}h^j$ with new auxiliary variables $\kappa^{1j}_t, \kappa^2_{ij} \ge 0$, respectively. The linearized constraints for all $\mathcal{J}$ are:

$$\begin{aligned}
&\kappa^{1j}_t \le Mz^j_t, \forall\, t \in \{k^L_j, ...k^U_j\}, j \in \mathcal{J} && \kappa^2_{ij} \le Mx_{ij}, \forall\, i \in \mathcal{M}_j, j \in \mathcal{J} \\
&\kappa^{1j}_t \le h^j, \forall\, t \in \{k^L_j, ...k^U_j\}, j \in \mathcal{J} && \kappa^2_{ij} \le h^j, \forall\, i \in \mathcal{M}_j, j \in \mathcal{J} \\
&\kappa^{1j}_t \ge h^j - M(1-z^j_t), \forall\, t \in \{k^L_j, ...k^U_j\}, j \in \mathcal{J} && \kappa^2_{ij} \ge h^j - M(1-x_{ij}), \forall\, i \in \mathcal{M}_j, j \in \mathcal{J}
\end{aligned} \tag{A.19}$$

With (A.19), we overcome the nonlinear terms and subsequently come up with an MILP formulation with symmetry (MC-MCLP-MILP$^{\text{SB}}$) for the distributionally robust capacitated uncovering location problem (MC-MCLP-DR), which we show in Proposition EC.3.

Proposition EC.3. *The* MC-MCLP-DR *problem is equivalent to the following mixed 0-1 integer linear programming problem:*

$$\text{MC-MCLP-MILP}^{\text{SB}} : \min \gamma \tag{A.20a}$$

$$\begin{aligned}
\text{s.t. } & (\text{A.13a}) - (\text{A.13b}), \ (\text{A.16c}) \\
& 1 - \tau' \le Uh^j + k^L_j y_j + \sum_{t=k^L_j+1}^{k^U_j} \kappa^{1j}_t \\
& \qquad + \sum_{i \in \mathcal{I}} (\underline{a}_i l^j_i + \overline{a}_i m^j_i + \mu^a_i n^j_i + \mu^a_i o^j_i), \forall\, j \in \mathcal{J}
\end{aligned} \tag{A.20b}$$

$$(\text{A.5b}) - (\text{A.5e}), (\text{A.12d}) - (\text{A.12j}), (\text{A.18}), (\text{A.19}), \ (\boldsymbol{x}, \boldsymbol{y}, \boldsymbol{z}) \in \mathcal{X}, \tag{A.20c}$$

where $\gamma, \boldsymbol{\alpha}, \boldsymbol{\beta}, \boldsymbol{\lambda}, \tau, \boldsymbol{c}, \boldsymbol{e}, \boldsymbol{f}, \boldsymbol{g}, \boldsymbol{h}, \boldsymbol{l}, \boldsymbol{m}, \boldsymbol{n}, \boldsymbol{o}, \boldsymbol{\alpha}', \boldsymbol{\beta}', \boldsymbol{\lambda}', \tau', \boldsymbol{r}, \boldsymbol{s}, \boldsymbol{t}, \boldsymbol{z}, \boldsymbol{\kappa}^1, \boldsymbol{\kappa}^2$ *are auxiliary variables.*

EC.2.2.2 Symmetry breaking constraints

We introduce the symmetry breaking constraints. Assume there are two homogeneous disposable AED units stored in one opened location with a maximum capacity of 3. The solutions $z_j = [1,1,0], z_j = [0,1,1], z_j = [1,0,1]$ are equivalent (i.e., with the same objective value). To avoid exploring for such equivalent solutions, we observe that the capacity is indexed sequentially with t; hence we can add constraints (A.21) to the linearized overall problem,

$$z^j_t \ge z^j_{t+1}, \forall\, t \in \{z^j_{L+1}, ..., z^j_U\}, j \in \mathcal{J}, \tag{A.21}$$

which enforces arbitrary ordering or scheduling of assigned disposable AED capacities. Constraints (A.21) are based on similar symmetry-breaking principles that used in Shehadeh et al. (2019), Shehadeh (2022). While breaking symmetry is important and standard in integer programming problems, to our knowledge, ours is the first attempt to break the symmetry in the solution space of the capacity allocation decisions of the capacitated covering location problem.

Recall that the available disposable AED assignment lies between k_j^L and k_j^U, and note that the maximal defibrillation demand can be an auxiliary upper bound of the available disposable AED assignment, and thus can be used to reduce the solution space. The maximal defibrillation demand in an area can be defined by $mdd{=}\sum_{i\in\mathcal{M}_j}\overline{a}^j, \forall\, j\in \boldsymbol{J}$. The gap between mdd and maximal disposable AED assignment can be defined as $(k_j^U-\max(mdd,k_j^L+1))^+$. The gap in location j leads to an affirmative number of empty assignments. The assignment index of empty disposable AED capacity is not affirmative. For example, suppose we can incorporate an empty disposable AED assignment index from 1 to 3. Then feasible solutions $(z^1=0,z^2=0)$, $(z^2=0,z^3=0)$, and $(z^1=0,z^3=0)$ yield the same objective value. To avoid exploring such equivalent solutions, we use an inverted order index as an empty assignment,

$$z_t^j=0, \forall\; t\in\{\max(mdd,k_j^L+1),...,k_j^U\}, j\in\mathcal{J}. \tag{A.22}$$

EC.2.3 Valid BigM values as upper bounds of $\boldsymbol{h}$

Recall we use BigM in both (A.15) and (A.19). We derive the bound of BigM values in these two inequalities. With the bound, the correlated linearized relaxation models MC-MCLP-MILP and MC-MCLP-MILP$^{\mathrm{SB}}$ are therefore more restricted, and easier to solve.

BigM is a sufficiently large number, which can be used in defining logic condition constraints. A BigM logic constraint is often used to linearize bilinear terms when one or two variables are binary. This method works in a nonlinear term, but due to the difficulty of finding a sufficiently large number, researchers generally use trial and error. Therefore, the linearized model normally performs badly in computing. The feasible solution space of a linearized model is adjusted with a BigM value. A lower BigM value is key to a linearized model. Fortunately, by exploring the model structure and prior information, the upper bound of the BigM value can be obtained Li et al. (2022).

In our model, we introduce BigM to linearize the bilinear term that contains $\boldsymbol{h}$; the upper bound cannot be obtained directly from variation and operation in the inequality. Instead, we solve an optimization problem related to the decision of demand and capacity allocation. We give the valid inequality of $\boldsymbol{h}$, which exactly captures the upper bound of auxiliary variable $\boldsymbol{h}$. With this bound, we have a minimally sufficient large number of $\boldsymbol{h}$. Since we directly use the valid inequality of auxiliary variables, this is the best relaxation under BigM linearization. The bound of h^j satisfies

$$0\le h^j\le \overline{h}^j,\; \overline{h}^j:=\frac{\overline{\triangle}_j}{\min_{\boldsymbol{x}_j,k_j}(\sum_{i\in\mathcal{M}_j}\overline{a}_i x_{ij}-U-k_j)^+}\;\forall\; j\in\mathcal{J}$$

$$\overline{\triangle}_j = \max_{\lambda_i',\alpha_i',\beta_i',\tau'} \left\{ \sum_{i\in\mathcal{I}} \left[(\overline{a}_i - \mu_i^a)\lambda_i' + \overline{a}_i(\alpha_i' + \beta_i') \right] - 1 + \tau' \right\} = \sum_{i\in\mathcal{I}} \left(\frac{\overline{a}_i - \mu_i^a}{\delta_i} + \frac{\overline{a}_i}{\overline{\mu}_i - \mu_i^a} + \frac{\underline{\mu}_i}{\mu_i^a - \underline{\mu}_i} \right).$$

We can use the obtained value $\overline{h}^j$ to replace the BigM value M in MC-MCLP-MILP and MC-MCLP-MILP$^{\text{SB}}$. Our paper's technique on BigM computing differs from Li et al. (2022). The major difference is that our auxiliary upper bound inequality not only based on variable bound information but also inequalities cross adding and deleting as well as two small optimization problems.

EC.3 Numerical experiments

We have applied a novel combination of various acceleration methods (as detailed in Section EC.2 in the e-companion) to significantly improve the computational tractability of our model formulated in Section 3. Based on these preparations, we now conduct an extensive empirical study. In Section EC.3.1, we explore the impact of parameters in the proposed MC-MCLP-DR model.

All experiments were programmed using Python 3.8. Optimization problems were solved using Gurobi 9.0 with a maximum time limit of one hour and run on a desktop computer with an Intel Core i5-4790K 4.0-GHz processor and 32 GB of RAM.

EC.3.1 Impact of DRO model parameters

We test small instances (8 areas, 5 candidate facilities) using the MC-MCLP-MILP model with a BigM value of 1000. The ambiguity set parameter settings are: $\underline{\boldsymbol{\mu}} = \underline{\boldsymbol{a}} = [5_8]^\top$, $\overline{\boldsymbol{\mu}} = [20,20,25,25,25,25,50,50]^\top$, $\overline{\boldsymbol{a}}= [35,35,40,40,40,40,100,100]^\top$, $\boldsymbol{\mu}^a = [10,10,15,15,15,15,20,20]^\top$, $\underline{k}_j$=30, $\overline{k}_j$=50, $\forall j \in \mathcal{J}$, δ_i=1, $\forall\ i \in \mathcal{I}$. We assume each facility could cover all demand areas, i.e., $\mathcal{M}_j = \mathcal{I}, \forall j \in \mathcal{J}$.

Impact of ambiguity set parameters on solution structure: We set $R_0 = 0.95$ and $U = 1$ as default parameter, and consider perturbations on parameters $(\overline{\boldsymbol{a}}, \underline{\boldsymbol{a}}, \overline{\boldsymbol{\mu}}, \underline{\boldsymbol{\mu}}, \boldsymbol{\delta})$. For $K \in \{100, 150\}$, we shrink the range of demand support bound from $[\underline{\boldsymbol{a}}, \overline{\boldsymbol{a}}]$ to $[\underline{\boldsymbol{a}}(1+\Delta_a), \overline{\boldsymbol{a}}(1-\Delta_a)]$ with $\Delta_a \in \{0, 0.1, 0.2, 0.3\}$, and shrink the range of expected demand volume $[\underline{\boldsymbol{\mu}}, \overline{\boldsymbol{\mu}}]$ to $[\underline{\boldsymbol{\mu}}(1+\Delta_\mu), \overline{\boldsymbol{\mu}}(1-\Delta_\mu)]$ with $\Delta_\mu \in \{0, 0.5, 0.6, 0.7\}$, respectively. In terms of $\boldsymbol{\delta}$, we decrease $\boldsymbol{\delta}$ to $\boldsymbol{\delta}(1-\Delta_\delta)$ with $\Delta_\delta \in \{0, 0.3, 0.4, 0.5\}$ for $K \in \{100, 150\}$. Notice that increasing the value of Δ ($\Delta_a, \Delta_\mu, \Delta_\delta$) makes the information of the ambiguity set more *precise*, as the range of the distribution parameter is narrowed and the number of candidate distributions is reduced correspondingly. Table EC.1 shows how capacity assignments and objective value vary with perturbations on $(\overline{\boldsymbol{a}}, \underline{\boldsymbol{a}}, \overline{\boldsymbol{\mu}}, \underline{\boldsymbol{\mu}}, \boldsymbol{\delta})$.

We see from Table EC.1 that, the perturbations on the parameters $(\overline{\boldsymbol{a}}, \underline{\boldsymbol{a}}, \overline{\boldsymbol{\mu}}, \underline{\boldsymbol{\mu}}, \boldsymbol{\delta})$ influence both the optimal capacity assignments and the objective value. More specifically, as Δ_a or Δ_μ increases, the disposable AED capacity is reassigned in each facility to meet the variation. One interesting finding is that increasing Δ enlarges the feasible solution set. This is contrary to what we expect, as it is commonly assumed that by increasing Δ, the number of candidate demand distribution

Table EC.1 Capacity allocation with perturbations on $(\overline{a}, \underline{a},\ \overline{\mu}, \underline{\mu}, \delta)$

		$\Delta_a(\overline{\boldsymbol{a}}, \underline{\boldsymbol{a}})$				$\Delta_\mu(\overline{\boldsymbol{\mu}}, \underline{\boldsymbol{\mu}})$				$\Delta_\delta(\boldsymbol{\delta})$			
		0	0.1	0.2	0.3	0	0.5	0.6	0.7	0	0.3	0.4	0.5
K=100	L_1	30	45	30	35	30	0	31	0	30	0	0	0
	L_2	30	46	40	35	30	40	39	39	30	38	38	30
	L_3	0	0	0	0	0	30	0	31	0	0	0	30
	L_4	0	0	0	30	0	0	30	30	0	30	32	40
	L_5	39	0	30	0	39	30	0	0	39	30	30	0
# Covered areas		3	4	4	5	3	4	5	6	4	4	4	4
OBJ		75	64	64	53	75	66	56	42	75	73.5	73	72
K=150	L_1	30	49	40	35	30	30	39	32	30	0	31	30
	L_2	30	49	39	40	30	30	31	48	30	49	30	30
	L_3	30	0	0	40	30	30	32	32	30	31	31	30
	L_4	30	49	40	35	30	30	48	0	30	30	0	30
	L_5	30	0	31	0	30	30	0	32	30	30	49	30
# Covered areas		5	6	6	7	5	5	5	6	5	5	5	5
OBJ		53	42	32	21	53	52	46	34.5	53	52.1	51.8	41.5

decreases, thus excluding associated solution from the feasible set. Proposition EC.4 shows that shrinking the ambiguity set parameters enlarges the feasible solution set, and hence the objective value decreases accordingly.

PROPOSITION EC.4. *Shrinking the ambiguity set parameters enlarges the model's feasible set.*

Impact of total disposable AED capacity and backup disposable AED resources on objective value. Let us analyse the impact of disposable AED capacity K, no stockout level R_0, and backup disposable AEDs U on the objective value. Table EC.2 illustrates how objective value vary with $K = \{100, 150\}$ $R_0 = \{0.5, 0.8, 0.9, 0.95, 0.98, 1\}$, and $U = \{1, 10, 20, 30\}$. In Table EC.2, as expected, the objective value decreases with K and U and increases with R_0, since increasing K and U or decreasing R_0 will enlarge the model's feasible solution space of the model. We observe that the optimal objective value does not change with K and U when K and U are large enough, since in this case the objective value is constrained by other resources such as R_0. Additionally, this experiment demonstrates that backup disposable AEDs U are less efficient than total capacity K. When $R_0 = 0.8$ and $K = 100$, at least 2 facilities will open due to the maximal quantity of capacity assignment $\overline{k}_j = 50$. In this case, the objective value is achieved at 11 when $U = 30$, which means backup disposable AEDs cost at least 60. When $K = 150$ and the objective value is 11, we will need at most 5 backup disposable AEDs. Therefore, the extra 150-100=50 capacities work more efficiently than the additional 60-5=55 backup disposable AEDs. In addition, this result is confirmed in the case study in Section 4 by fixing the value of $K + \sum_{j \in \mathcal{J}} U * y_j$ and varying the values of K and U.

Table EC.2 Objective value of MC-MCLP-MILP with different values of K, U, and R_0

	K=100												K=150											
$R_0 =$	0.1	0.2	0.3	0.4	0.5	0.6	0.7	0.8	0.9	0.95	0.98	1	0.1	0.2	0.3	0.4	0.5	0.6	0.7	0.8	0.9	0.95	0.98	1
$U = 1$	37	38	42	42	43	48	54	64	74	75	80	80	0	0	11	11	16	22	27	38	43	53	53	53
$U = 10$	16	21	21	22	32	37	43	53	59	64	64	64	0	0	0	0	0	0	0	11	22	32	42	42
$U = 20$	0	0	0	0	11	11	16	21	32	42	42	42	0	0	0	0	0	0	0	0	0	21	42	42
$U = 30$	0	0	0	0	0	0	0	11	21	32	42	42	0	0	0	0	0	0	0	0	0	0	21	42

Impact of no stockout levels and disposable AED resources on marginal objective value. We also formulate the marginal value of the objective function and compare it with conclusions. We first obtain the difference value between each range of $R_0, e.g., 0.5-0.6$, and then the value is divided by the multiple of that range over unite range 0.1, e.g., the multiple of $0.5-0.6$ is $0.1/0.1=1$. And the marginal value is obtained by the difference value between objective value given R_0, i.e., $48-43=5$ divided by the multiple value 1 equals to 5. Then the marginal value is computed based on Table EC.2 and logged in Table EC.3.

Table EC.3 Marginal objective values of MC-MCLP-MILP with different values of K, U, and R_0

	K=100								K=150							
$R_0 =$	0.5-0.6	0.6-0.7	0.7-0.8	0.8-0.9	0.9-1	0.9-0.95	0.95-0.98	0.98-1	0.5-0.6	0.6-0.7	0.7-0.8	0.8-0.9	0.9-1	0.9-0.95	0.95-0.98	0.98-1
$U=1$	5	6	10	10	6	2	16.7	0	8	5	11	32	10	20	0	0
$U=10$	5	6	6	6	5	10	0	0	-	-	-	11	20	20	33	0
$U=20$	0	5	5	11	10	20	0	0	-	-	-	-	-	-	70	0
$U=30$	-	-	-	10	21	22	33.3	0	-	-	-	-	-	-	-	105

Where '-' denote there exits no marginal value in current range of R_0. This appears in two cases, (1) a range where objective values equals zero (2) a range where objective value initially not equals to zero

We call a range of R_0 as a *variation scope* if the marginal value is larger than zero when R_0 is in this range. For example, in Table EC.3, when $K=100$ and $U=30$, a variation scope of R_0 is $[0.8, 0.98]$. Using the definition, we find that the length of variation scope of R_0 decreases with U or K, e.g., given $U=30$, the length of variation scope decreases from 0.18 to 0.02 when K increases from 100 to 150. This observation is fairly natural since the risk of stockout is hedged when more disposable AEDs are available. In addition, we notice that, as the increase of R_0, the marginal objective increases slowly first, then rapidly, and then slowly. In other word, the marginal value is sensitive to the middle part of the variation scope, and less sensitive to the two tail parts of the variation scope.

EC.3.2 In-sample verification

Our in-sample results are consistent with the ones obtained in numerical experiments. More specifically, we conducted similar experiments on the DRO model as in Section EC.3.1. In this experiment, we vary the summation of total capacity and backup volume $\Theta := K + \sum_{j \in \mathcal{J}} U * y_j = \{80, 240, 400\}$ (This can be realized by adding an additional constraint in MC-MCLP-MILP$^{\text{SB}}$). in the DRO model. Concurrently, we change the parameters of $U = \{15, 30, 45\}$ and $R_0 = \{0.1, 0.2, ..., 1\}$ to observe their impact on the objective value. The results are summarized in Figure EC.1.

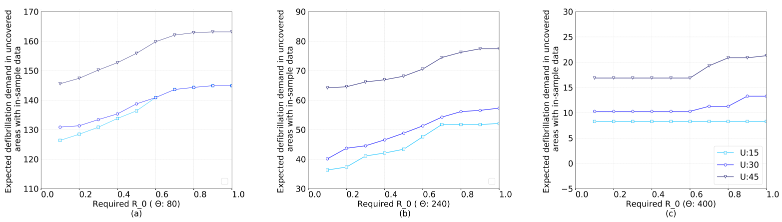

Figure EC.1 In-sample system parameter impact on objective value.

Figure EC.1 highlights that the total capacity has a more pronounced impact than the backup volume. As U increases from 15 to 45, K decreases accordingly as Θ is fixed, while the objective value increases. Additionally, we observe that the objective value is particularly sensitive to variations in R_0 when it approaches mid-range levels, such as 0.4-0.8 in Figure EC.1 (a), 0.7-0.9 in Figure EC.1 (b), and 0.6-0.8 in Figure EC.1 (c). Conversely, sensitivity to variations in R_0 diminishes when R_0 is relatively small or large. Another noteworthy finding is that the objective value remains constant with changes in R_0 when the backup volume is set to 15, as illustrated in Figure EC.1 (c). Figure EC.1 (c) presents a scenario where the objective value remains unaffected by the probability of no stockout. This can be attributed to the total capacity being sufficiently ample to maintain high no-stockout probabilities without compromising demand fulfillment in covered areas.

EC.4 Hypothesis test of OHCA cases for Poisson distribution

The hypothesis test of the OHCA data is performed following the Chi-squared goodness-of-fit. We select the years 2017, 2018, and combined 2017-2018 data as sample datasets. The hypothesis test procedure is summarized as follows. We use the 2017 data to illustrate the procedure in (a)–(d), and then apply exactly the same method to the 2018 and combined 2017-2018 datasets in (e).

(a) First sort the data and obtain a frequency of daily OHCA cases, the daily OHCA cases frequency data is deemed as a benchmark observation. Based on this observation, we verify if the potential empirical distribution follows a Poisson distribution as assumed in (Boutilier and Chan 2022).

(b) Assume the observation sample follows a Poisson distribution, thus the sample means $\hat{\lambda}$ can form a theoretical empirical Poisson distribution where variance and mean are all $\hat{\lambda}$. In this way, we can describe the empirical Poisson based on $\hat{\lambda}$ and performs the result of theoretical inferred value in each event contained in previous observations.

(c) We then compare the observation and inferred value to check if there are belongs to the same distribution. To this end, we perform a Chi-squared test with H0: the OHCA's daily demand in the year 2017 follows a Poisson distribution, and H1: the OHCA's daily demand in the year 2017 not follows a Poisson distribution. In particular, some results can be found in the following.

Table EC.4 Observation samples and the inferred value based on a Poisson assumption where $\hat{\lambda} = 2.616$

Daily OHCA	0	1	2	3	4	5	6	7	8	9	10
Observations	31	76	99	54	51	26	18	5	4	0	1
Inferred Prob.	0.07	0.19	0.20	0.22	0.143	0.0747	0.033	0.012	0.004	0.0012	0.0003
Inferred Value	26.67	69.8	91.3	79.6	52.1	27.2	11.9	4.4	1.5	0.4	0.1

We compute the empirical probability mass function for a number of cases in one day and have the inferred value vector for the daily OHCA cases from $0-10$. empirical probability and the correlated inferred value vector is in Table EC.4.

(d) Result and conclusion (for the year 2017). We apply the Chi-squared goodness of fit of two frequency vectors, we apply the scipy.stats module and obtained the chi-squared test statistic 25.49 and the p value is $0.0044 < 0.05$. Since the p-value is less than 0.05, we successfully reject the null hypothesis. This means we have sufficient evidence to say that the distribution of a number of daily OHCA cases from observations is not a Poisson thus contrary to the distributional assumption that the MSOM paper had claimed.

(e) Results for the 2018 and combined 2017-18 datasets: We repeated the same hypothesis testing procedure for the 2018 dataset and the combined 2017-2018 dataset (see the observed and expected values in Table EC.5). The sample mean for the 2018 dataset was $\hat{\lambda} = 3.05$ and for the combined dataset was $\hat{\lambda} = 2.84$. The Chi-squared test for the 2018 dataset yielded a test statistic of 161.94 and a p-value of $2.10e-10$. Similarly, the test for the combined 2017-2018 dataset produced a test statistic of 178 and a p-value of $1.08e-10$. The exceptionally small p-value for the 2018 dataset (and the combined dataset) indicates a severe lack of fit. This is likely due to over dispersion in the data, where the observed variance far exceeds the mean, indicating that the Poisson distribution cannot accommodate emergency service demand.

Consistent with the results for 2017, the p-values for both the 2018 dataset and the combined 2017-2018 dataset were less than 0.05. Therefore, we reject the null hypothesis for these datasets as well. This provides further evidence that the Poisson distribution may not be an appropriate assumption for the daily demand for OHCA services in this context.

Table EC.5 Observation samples and the inferred value based on a Poisson assumption

Dataset	$\hat{\lambda}$	Daily OHCA	0	1	2	3	4	5	6	7	8	9	10	11	12
		Observations	51	53	60	70	39	40	25	8	9	5	3	1	1
Y-2018	3.05	Inferred Prob.	0.05	0.14	0.22	0.22	0.17	0.10	0.05	0.02	0.01	0.00	0.00	0.00	0.00
		Inferred Value	17.20	52.55	80.27	81.74	62.42	38.14	19.42	8.47	3.24	1.10	0.34	0.09	0.02
		Observations	82	129	158	125	90	66	43	13	13	5	4	1	1
Combined	2.84	Inferred Prob.	0.06	0.17	0.24	0.22	0.16	0.09	0.04	0.02	0.01	0.00	0.00	0.00	0.00
		Inferred Value	42.78	121.37	172.16	162.80	115.47	65.52	30.98	12.55	4.45	1.40	0.40	0.10	0.02

EC.5 Congestion experiments: Toronto case

Table EC.6 OHCA response comparison under congestion: RTI+mean vs. covering models

Solutions of RTI+mean model			**Performance of drone delivery** # of OHCA cases within (x) mins								**Deployment under covering model**		**Performance of drone delivery** # of OHCA cases within (x) mins							
γ	# drones	# AEDs	8	7	6	5	4	3	2	1	*Drones*	*AEDs*	8	7	6	5	4	3	2	1
1	5	77	75	72	70	64	48	36	11	2	(5)	(77)	77	77	77	77	65	55	27	6
2	9	225	219	207	189	161	138	119	79	27	(4,5)	(114,111)	225	225	225	224	197	137	84	24
3	16	369	365	358	344	318	294	236	168	54	(1,5,5,5)	(3,75,81,209)	365	365	365	365	339	257	116	40

We assume a population density for Toronto that is 12 times that of VBC.

EC.5.1 Comparison of MAD-DRO with type-1 and type-∞ DRO

As shown in Table EC.8, our Mean-Absolute Deviation DRO (MDRO) model achieves effectiveness comparable to the 1-WDRO and ∞-WDRO models, as indicated by the similar quantities of OHCA

Table EC.7 OHCA response comparison under congestion: RTI+CVaR vs. covering models

	Solutions of RTI+mean model		Performance of drone delivery # of OHCA cases within (x) mins								Deployment under covering model		Performance of drone delivery # of OHCA cases within (x) mins							
γ^{90}	# drones	# AEDs	8	7	6	5	4	3	2	1	*Drones*	*AEDs*	8	7	6	5	4	3	2	1
10%	5	116	89	80	63	43	30	24	7	3	(5)	(115)	115	115	115	114	100	68	45	8
20%	8	187	168	145	112	74	52	38	20	4	(4,4)	(96,91)	187	187	187	186	164	84	39	12
30%	12	280	255	225	177	124	87	62	33	9	(5,4,4)	(74,140,66)	280	280	280	278	241	185	87	18

We assume a population density for Toronto that is 12 times that of VBC.

patients served within 6, 5, and 4 minutes. Furthermore, Tables EC.9 and EC.10 show that the MDRO model yields a smaller performance gap between urban and non-urban areas, indicating a reduced resource imbalance between these regions. (The definitions of “urban” and “non-urban” are provided later in Section 4.5.2, and the performance gap is detailed in Section 4.5.3.) For this experiment, we kept the backup volume at its minimum value of 1.

Table EC.8 In sample model effectiveness comparison: MDRO, 1-WDRO, ∞-WDRO.

	AEDs deployment	Performance: OHCA cases within (x) mins				AEDs deployment	Performance: OHCA cases within (x) mins				AEDs deployment	Performance: OHCA cases within (x) mins			
(P,K)	MDRO	6	5	4	3	1-WDRO	6	5	4	3	∞-WDRO	6	5	4	3
(250,4)	(74, 68, 61, 47)	250	250	234	178	(72, 51, 71, 56)	246	246	229	199	(72, 51, 68, 56)	243	243	229	199
(350,5)	(56, 74, 72, 44, 103)	340	338	283	203	(72, 51, 85, 77, 56)	330	330	310	260	(72, 61, 85, 76, 56)	339	339	320	260

Note: We keep all other parameters the same, such as R_0, U.

Table EC.9 Out of sample model fairness comparison: MDRO, 1-WDRO, ∞-WDRO. (P,K)= (250,4)

	MDRO Performance improvement (%)					1-WDRO Performance improvement (%)					∞-WDRO Performance improvement (%)				
Patient class ↓ Perturbation →	0%	10%	20%	30%	40%	0%	10%	20%	30%	40%	0%	10%	20%	30%	40%
Urban	52.64	50.10	49.02	47.89	46.96	53.54	50.92	49.77	48.58	47.60	53.43	50.82	49.67	48.49	47.52
Sub-urban	32.08	29.31	31.75	30.77	32.86	22.64	20.69	23.81	23.08	25.71	18.87	17.24	20.63	20.00	22.86
Performance gap	20.56	20.79	17.27	17.12	14.10	30.90	30.23	25.96	25.50	21.89	34.56	33.58	29.04	28.49	24.66

Note: Threshold = 6 min, we keep all other parameters the same, such as R_0, U. We did not compare the performance of OHCA cases within (x) mins in out of sample as it performs quite similar to that in-sample experiments.

Table EC.10 Out of sample model fairness comparison: MDRO, 1-WDRO, ∞-WDRO. (P,K) = (350,5)

	MDRO Performance improvement (%)					1-WDRO Performance improvement (%)					∞-WDRO Performance improvement (%)				
Patient class ↓ Perturbation →	0%	10%	20%	30%	40%	0%	10%	20%	30%	40%	0%	10%	20%	30%	40%
Urban	56.36	53.48	52.10	50.73	49.60	58.04	56.13	54.82	53.23	51.92	57.82	55.93	54.63	53.06	51.76
Sub-urban	35.85	32.76	34.92	33.85	35.71	35.85	32.76	34.92	33.85	35.71	37.74	34.48	36.51	35.38	37.14
Performance gap	20.51	20.72	17.18	16.88	13.89	22.19	23.37	19.90	19.38	16.21	20.08	21.45	18.12	17.68	14.62

Note: We test under the 6 min threshold and keep all other parameters the same, such as R_0, U.

To summarize, the performance tables indicate that WDRO has similar effectiveness to MAD-DRO in our studied MC-MCLP. Similar result can be found in the recent study by Fu et al. (2024). In addition, we omit the moment-based DRO, since our results show that moment-based DRO shows significant conservative solutions compared with WDRO and MDRO.

EC.6 Original dataset and updated dataset

In our experiment, we use dataset from Custodio and Lejeune (2022). The original dataset is shown in the left side (a) of Figure EC.2. It is evident that over 300 response time entries are recorded as zero, a value that reflects missing or invalid. Based on the rationale and initial response time processing workflow described in Custodio and Lejeune (2022), these zero values were updated with corresponding historical response times (taken from the first response time of a fire, hospital, or police station). The original non-zero response time values from the 2017 dataset were used as a test set, resulting in a replication accuracy exceeding 97%. The updated dataset, OHCA2025updated.xlsx, is available via the associated GitHub repository. All code we developed to merge and update the data sets are available in the online repository (`https://github.com/zhangrun20180405/MCLP-revision-experiments`).

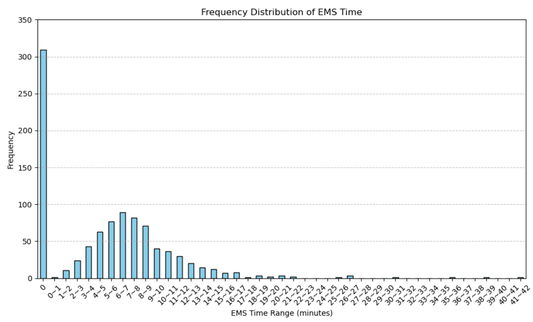

(a) Y 2017 response time frequency

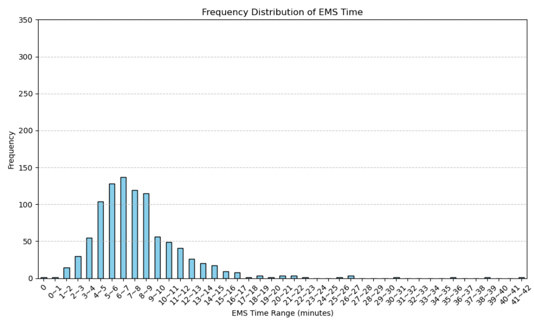

(b) Updated response time frequency

Figure EC.2 Original vs. Updated Dataset: Frequency Distribution

The right side (b) of Figure EC.2 illustrates the updated response time distribution. Both datasets have 955 records. The original dataset (mean = 5.40, Q1 = 0.00) includes many very low values, while the updated one (mean = 7.75, Q1 = 5.28) shows few extreme lows.

Table EC.11 Comparison of statistical descriptions between two datasets

Dataset	Count	Mean	Median	Std. Dev.	Max	Q1 (25%)	Q3 (75%)	90%
Original	955	5.40	5.37	5.21	41.12	0.00	8.33	11.35
Updated	955	7.75	7.05	4.00	41.12	5.28	9.20	12.20

As in Table EC.12 the covering model outperforms the RTI+CVaR when without data update. Similar results related to fairness are in Tables EC.13 and EC.14.

Table EC.12 Comparison of OHCA drone response effectiveness: RTI+CVaR vs. covering models

	Solutions of RTI+CVaR model		Performance of drone delivery # of OHCA cases within (x) mins								Solutions of covering model		Performance of drone delivery # of OHCA cases within (x) mins							
γ^{90}	# bases	# AEDs	8	7	6	5	4	3	2	1	# bases	# AEDs	8	7	6	5	4	3	2	1
10%	2	109	95	84	61	37	29	23	13	2	2	109	109	109	109	109	101	83	36	6
20%	3	180	151	130	103	80	51	30	14	1	3	180	180	180	180	180	162	135	45	18
30%	3	328	298	272	210	134	101	71	41	13	3	328	328	328	328	327	292	212	88	24

γ^{90}: the proportion by which the 90th percentile value is reduced. Dataset is the original dateset.

EC.7 Proof of equality between maximum covering and minimum uncover objective function

We show that these two objective function are mathematically equivalent. Let $\tilde{a}_i$ denote (possibly uncertain) defibrillation demand at area i, and let x_{ij} indicate whether demand area i is assigned

Table EC.13 Comparison of OHCA drone response fairness: RTI+mean vs. covering models

	Solutions of RTI+mean model		**Improvement of non-urban areas** # of OHCA cases within (x) mins								**Solutions of covering model**		**Improvement of non-urban areas** # of OHCA cases within (x) mins							
γ	# bases	# AEDs	8	7	6	5	4	3	2	1	# bases	# AEDs	8	7	6	5	4	3	2	1
0	0	0	178	159	135	120	103	96	91	89	0	0	178	159	135	120	103	96	91	89
1	2	75	+15	+15	+10	+4	+4	+3	+1	+1	2	75	+15	+21	+23	+25	+26	+22	+19	+11
2	3	188	+48	+44	+31	+13	+10	+5	+1	+1	3	188	+19	+26	+31	+32	+35	+27	+9	+1
3	3	273	+62	+56	+40	+16	+13	+8	+1	+1	3	273	+26	+34	+41	+43	+39	+26	+10	+1

dataset: original dataset.

Table EC.14 Comparison of OHCA drone response fairness: RTI+CVaR vs. covering models

	Solutions of RTI+CVaR model		**Improvement of non-urban areas** # of OHCA cases within (x) mins								**Solutions of covering model**		**Improvement of non-urban areas** # of OHCA cases within (x) mins							
γ^{90}	# bases	# AEDs	8	7	6	5	4	3	2	1	# bases	# AEDs	8	7	6	5	4	3	2	1
0	0	0	178	159	135	120	103	96	91	89	0	0	178	159	135	120	103	96	91	89
10%	2	109	+43	+35	+19	+3	+2	+2	+0	+0	2	109	+4	+7	+7	+7	+9	+10	+7	+1
20%	3	180	+64	+58	+42	+29	+14	+6	+4	+1	3	180	+18	+28	+31	+34	+37	+34	+9	+1
30%	3	328	+83	+83	+54	+13	+10	+5	+0	+0	3	328	+37	+51	+60	+64	+53	+36	+11	+1

dataset: original dataset.

to facility j (feasible only when the critical time window and capacity constraints are satisfied). Consider the objective function of the MC-MCLP-DR problem discussed in our manuscript.

$$\min_{(\boldsymbol{x},\boldsymbol{y},\boldsymbol{k})\in\mathcal{X}} \sup_{\mathbb{P}\in\mathcal{G}} \mathbb{E}_{\mathbb{P}} \sum_{i\in\mathcal{I}} \tilde{a}_i (1 - \sum_{j\in\mathcal{N}_i} x_{ij})$$

The original objective can be rewritten as

$$\sup_{\mathbb{P}\in\mathcal{G}} \mathbb{E}_{\mathbb{P}} \left[\sum_{i\in\mathcal{I}} \tilde{a}_i \right] - \max_{(\mathbf{x},\mathbf{y},\mathbf{k})\in\mathcal{X}} \inf_{\mathbb{P}\in\mathcal{G}} \quad \mathbb{E}_{\mathbb{P}} \left[\sum_{i\in\mathcal{I}} \tilde{a}_i \sum_{j\in\mathcal{N}_i} x_{ij} \right].$$

Here, the first term independent to the decisions, thus minimizing the expected unallocated demand is equivalent to maximizing the worst-case expected on-time (covered) demand.

References

[EC80] Li J, Wang S, Li Y (2022) Redundancy allocation under state-dependent distributional uncertainty of component lifetimes. Technical report, University of Chinese Academy of Sciences, working paper.

[EC81] Shehadeh KS (2022) Distributionally robust optimization approaches for a stochastic mobile facility fleet sizing, routing, and scheduling problem. *Transportation Science* .

[EC82] Shehadeh KS, Cohn AE, Epelman MA (2019) Analysis of models for the stochastic outpatient procedure scheduling problem. *European Journal of Operational Research* 279(3):721–731.